

1 **Revised treatment of wet scavenging processes dramatically improves GEOS-Chem**
2 **12.0.0 simulations of surface nitric acid, nitrate, and ammonium over the United**
3 **States**

4
5 Gan Luo, Fangqun Yu, and James Schwab
6 Atmospheric Sciences Research Center, University at Albany

7
8 **Abstract**

9 The widely used community model GEOS-Chem 12.0.0 and previous versions have
10 been recognized to significantly overestimate the concentrations of gaseous nitric acid,
11 aerosol nitrate, and aerosol ammonium over the United States. The concentrations of
12 nitric acid are also significantly over-predicted in most global models participating a
13 recent model inter-comparison study. In this study, we show that most or all of this
14 overestimation issue appears to be associated with wet scavenging processes.
15 Replacement of constant in-cloud condensation water (ICCW) assumed in GEOS-Chem
16 standard versions with one varying with location and time from the assimilated
17 meteorology significantly reduces mass loadings of nitrate and ammonium during the
18 wintertime, while the employment of an empirical washout rate for nitric acid
19 significantly decreases mass concentrations of nitric acid and ammonium during the
20 summertime. Compared to the standard version, GEOS-Chem with updated ICCW and
21 washout rate significantly reduces the simulated annual mean mass concentrations of
22 nitric acid, nitrate, and ammonium at surface monitoring network sites in US, from 2.04
23 to 1.03 $\mu\text{g m}^{-3}$, 1.89 to 0.88 $\mu\text{g m}^{-3}$, 1.09 to 0.68 $\mu\text{g m}^{-3}$, respectively, in much better
24 agreement with corresponding observed values of 0.83, 0.70, and 0.60 $\mu\text{g m}^{-3}$,
25 respectively. In addition, the agreement of model simulated seasonal variations of
26 corresponding species with measurements is also improved. The updated wet scavenging
27 scheme improves the skill of the model in predicting nitric acid, nitrate, and ammonium

1 concentrations which are important species for air quality and climate.

1 **1. Introduction**

2 Nitrate and ammonium are important secondary inorganic aerosols in the
3 atmosphere, contributing significantly to total aerosol mass over most polluted regions
4 (Bian et al., 2017) and to aerosol direct radiative forcing over urban and agriculture
5 regions (Bauer et al., 2007; Myhre et al., 2013). The amount of nitrate and ammonium
6 also regulates the concentration of gaseous ammonia which often plays an important role
7 in the formation of new particles (Kirkby et al., 2011; Yu et al., 2018). In addition, nitrate
8 and ammonium help newly formed particles grow to larger sizes suitable for cloud
9 condensation nuclei (Yu and Luo, 2009) and thus can impact aerosol indirect radiative
10 forcing (Twomey, 1977).

11 Nitric acid, nitrate, and ammonium concentrations are often overestimated by
12 atmospheric models (Pye et al., 2009; Walker et al., 2012; Bian et al., 2017; Zakoura and
13 Pandis, 2018), including the widely used community model GEOS-Chem (e.g., Zhang et
14 al., 2012; Heald et al., 2012). Zhang et al. (2012) studied nitrogen deposition over the US
15 with GEOS-Chem and found both nitric acid and nitrate concentrations are overestimated,
16 especially in wintertime. They suggested that this is the result of excessive nitric acid
17 formation via night time chemistry of heterogeneous N_2O_5 hydrolysis. However, Heald et
18 al. (2012) found the overestimate of heterogeneous N_2O_5 hydrolysis does not fully
19 account for the nitrate bias and suggested the positive nitrate bias is likely linked with an
20 overestimate of nitric acid concentrations. Heald et al. (2012) investigated other possible
21 causes for the overestimation of nitric acid concentrations arising from uncertainties in
22 daytime formation and dry deposition, and concluded that none of these uncertainties
23 could fully account for the reduction in nitric acid required to correct the nitrate bias.
24 Based on comparisons of simulated nitrate and ammonium aerosol from nine
25 AEROCOM models with ground station and aircraft measurements, Bian et al. (2017)
26 concluded that most models overestimate surface nitric acid volume mixing ratio by a
27 factor of up to 3.9 over North America and the overestimation cannot be simply attributed

1 to model uncertainties. Backes et al. (2016) suggested that uncertainties in the temporal
2 profiles of ammonia emissions could also contribute significantly to the bias of nitrate
3 concentrations. However, the impact of ammonia mostly happened during summer time.
4 Zakoura and Pandis (2018) found significant decrease in nitrate concentration when they
5 enhanced their model resolution from $36 \text{ km} \times 36 \text{ km}$ to $4 \text{ km} \times 4 \text{ km}$ in the PMCAMx
6 model. However, similar results are not found in global models with much coarser grids
7 than regional models. All these studies indicate that the overestimation of nitric acid,
8 nitrate, and ammonium mass concentrations in current atmospheric chemistry models
9 remains to be resolved.

10 In this study, we proposed an improved treatment of wet scavenging in GEOS-Chem
11 by considering cloud condensation water variability and empirical washout rate, which
12 together significantly improve the estimates of nitric acid, nitrate, and ammonium over
13 the US. GEOS-Chem is a global 3-D model of atmospheric chemistry driven by
14 meteorological input from the Goddard Earth Observing System (GEOS) of the NASA
15 Global Modeling and Assimilation Office and includes state-of-the-art routines to deal
16 with emissions, transport, and other key chemical and physical processes for atmospheric
17 trace gases and aerosols (Keller et al., 2014; Fontoukis and Nenes, 2007; Martin et al.,
18 2003; Bey et al., 2001). The improved wet scavenging in GEOS-Chem is described in
19 section 2. The comparison of model results with surface observations and the changes of
20 the three species over the US are presented in section 3. Section 4 is the summary and
21 discussion.

22

23 **2. Improved scheme for wet scavenging**

24 Wet scavenging is the main removal pathway for many atmospheric air pollutants.
25 Two mechanisms are involved in wet scavenging: rainout (in-cloud scavenging) and
26 washout (below-cloud scavenging). GEOS-Chem treats wet scavenging associated with
27 stratiform and convective precipitation separately. The wet deposition scheme in

1 GEOS-Chem is described by Jacob et al. (2000) and Liu et al. (2001) for water-soluble
 2 aerosols, and by Amos et al. (2012) for gases. Scavenging of aerosol by snow and
 3 cold/mixed precipitation is described by Wang et al. (2011, 2014). The first-order rainout
 4 parameterization is based on Giorgi and Chameides (1986).

6 **2.1 Impact of in cloud condensed water (ICCW)**

7 For stratiform precipitation, in the most recently released GEOS-Chem version
 8 12.0.0 (GC12), rainout water soluble species is parameterized according to Jacob et al.
 9 (2000) and Liu et al. (2001) as

$$10 \quad F = \frac{P_r}{k \cdot ICCW} (1 - e^{-k \cdot \Delta t}) \quad (1)$$

11 where F is the fraction of a water soluble tracer in the grid-box scavenged by rainout, Δt
 12 (s) is the model integration time step. k (s^{-1}) is the first-order rainout loss rate (Giorgi and
 13 Chameides, 1986) which represents the conversion of cloud water to precipitation water.
 14 $ICCW$ ($g \ m^{-3}$) represents the condensed water content (liquid) within the precipitating
 15 cloud (i.e., in cloud) and P_r ($g \ m^{-3} \ s^{-1}$) is the rate of new precipitation formation (rain only)
 16 in the corresponding grid-box.

17 The rainout loss rate (k) represents how fast cloud condensation water can be
 18 removed from the atmosphere and thus is critical for rainout scavenging. k is defined in
 19 Jacob et al. (2000) and coded in GC12 (called k_{GC12} thereafter) as

$$20 \quad k_{GC12} = k_{min} + \frac{P_r}{ICCW} \quad (2)$$

21 where k_{min} (s^{-1}) is the minimum value of rainout loss rate derived from the stochastic
 22 collection equation which indicates that in one hour at least ~ 0.36 of cloud droplets are
 23 lost to autoconversion/accretion (Beheng and Doms 1986). In GC12, k_{min} is set to be 0.36
 24 $hr^{-1} = 1 \times 10^{-4} \ s^{-1}$.

25 It should be noted that P_r in Eq. (2) is a grid-box mean value, while $ICCW$ is an in
 26 cloud value. To be physically consistent, we suggest a new expression of k (k_{new}) that
 27 replaces grid-box mean P_r with the corresponding in cloud value P_r/f_c .

$$1 \quad k_{new} = k_{min} + \frac{P_r}{f_c \cdot ICCW} \quad (3)$$

2 where f_c is the grid-box mean cloud fraction. As we will show later, Eq. (3) gives k values
 3 in much better agreement with those derived from cloud model simulations and
 4 observations.

5 To calculate F , GC12 uses P_r from the Modern-Era Retrospective analysis for
 6 Research and Applications Version 2 (MERRA2) meteorological fields. For $ICCW$ in Eqs.
 7 1-3, Jacob et al. (2000) used a constant value of 1.5 g m^{-3} and Wang et al. (2011) changed
 8 it to 1 g m^{-3} . In GC12, the default value of $ICCW$ is 1 g m^{-3} . However, $ICCW$ in the
 9 atmosphere varies with time and location. Here we suggest to use time and location
 10 dependent $ICCW$ (named $ICCW_t$) which can be derived from MERRA2 meteorological
 11 fields as

$$12 \quad ICCW_t = \frac{CW + P_r \cdot \Delta t}{f_c} \quad (4)$$

13 where CW is grid-box mean cloud water content, while $P_r \cdot \Delta t$ represents rain water
 14 content produced during the time step Δt . In a previous study, Croft et al. (2016) used
 15 cloud liquid and ice water content to replace the fixed $ICCW$. However, as shown in
 16 Equation 6 in MERRA2's file specification (Bosilovich et al., 2016), cloud water is the
 17 residual condensation water after precipitation and is low when precipitation is occurring.
 18 Because the fraction of soluble species rained out should equal to the fraction of total
 19 condensed water (or $ICCW$ in our case) converted to rain water, we think that $ICCW$ in
 20 Eq (3) should include rain water (i.e., Eq 4).

21 Figure 1a shows seasonal variations of $ICCW_t$ (Eq. 4) averaged throughout the lower
 22 troposphere (0–3 km) of the whole globe ($ICCW_{t,G}$), over all land surface ($ICCW_{t,L}$),
 23 over the oceans ($ICCW_{t,O}$), and over the continental US ($ICCW_{t,US}$). For comparisons, the
 24 constant values of $ICCW$ assumed in Jacob et al. (2000) ($ICCW_{J2000}$) and GC12
 25 ($ICCW_{GC12}$) are also shown. The monthly mean values of $ICCW_{t,G}$, $ICCW_{t,L}$, $ICCW_{t,O}$,

1 and $ICCW_{t_US}$ vary within the ranges of 0.90–1.03 g m⁻³, 0.30–0.45 g m⁻³, 1.15–1.26 g
 2 m⁻³, and 0.21–0.53 g m⁻³, respectively. This figure shows that $ICCW_{t_G}$ is close to the
 3 assumed $ICCW$ value of 1 g m⁻³ used in GC12. As can be seen from Fig.1a, $ICCW_{t_O}$ is
 4 greater than 1 g m⁻³, but $ICCW_{t_L}$ is much less than the constant value of 1 g m⁻³ assumed
 5 in GC12. The mean $ICCW$ over the continental US (bright green line) is close to $ICCW_{t_L}$
 6 (olive line), and is ~ 5 times less than the assumed value in GC12 during the wintertime
 7 and ~ 2 times less during the summertime. As we will show later, the constant $ICCW$ of 1
 8 g m⁻³ assumed in GC12 leads to significant underestimation of rainout over the
 9 continental US, especially during the wintertime.

10 Figure 1b shows seasonal variations of mean k_{GC12} , k_{new} , and $k_{new_ICCW_t}$ in the lower
 11 troposphere (0-3 km) of the continental US. Referring to Eq. (2), the figure shows that
 12 k_{GC12} is dominated by k_{min} (which is physically unsound) and thus shows negligible
 13 seasonal variation. Conversely, k_{new} is low in the wintertime and high in the
 14 summertime. $k_{new_ICCW_t}$ is 2.3 times higher than k_{new} during January and 1.6 times higher
 15 than k_{new} during July. Both k_{new} and $k_{new_ICCW_t}$ are within the range of rainout loss rates
 16 (10^{-4} – 10^{-3} s⁻¹) indicated by cloud model simulations and estimates based on observations
 17 (Giorgi and Chameides, 1986).

18 From Eqs. (1), (3), and (4), we can get the updated parameterization for rainout loss
 19 fraction at each location and time step

$$20 \quad F = \frac{f_c \cdot P_r}{k_{new_ICCW_t} (CW + P_r \cdot \Delta t)} \left(1 - e^{-k_{new_ICCW_t} \cdot \Delta t} \right) \quad (5)$$

21

22 **2.2 Impact of empirical washout rate on nitric acid wet scavenging**

23 Still considering the case of stratiform precipitation in GOES-Chem, the fraction of
 24 aerosols and HNO₃ within a grid-box that is scavenged by washout over a time step is
 25 parameterized as (Wang et al., 2011; Liu et al., 2001; Jacob et al., 2000)

1 $F_{wash} = f_r(1 - \exp(-k_{wash}\Delta t))$ (6)

2 $f_r = \max\left(\frac{P_r}{k \cdot ICCW}, f_{top}\right)$ (7)

3 $k_{wash} = \Lambda \left(\frac{P_r}{f_r}\right)^b$ (8)

4 where f_r is the horizontal areal fraction of the grid-box experiencing precipitation and f_{top}
5 is the value of f_r in the layer overhead ($f_{top} = 0$ at the top of the precipitating column).
6 k_{wash} is washout rate, Λ is washout scavenging coefficient, and b is an exponential
7 coefficient. In the original GEOS-Chem, $\Lambda = 1 \text{ cm}^{-1}$ and $b = 1$ for both aerosols and nitric
8 acid (Liu et al., 2001; Jacob et al., 2000).

9 It has been well recognized that, for aerosols, Λ and b depend on particle size (Wang
10 et al., 2010; Feng, 2007; Andronache et al., 2006; Henzing et al., 2006; Laakso et al.,
11 2003). Feng (2007) suggested values of $b = 0.62, 0.61,$ and 0.8 for particles in nucleation
12 (diameter $1 \text{ nm} - 40 \text{ nm}$), accumulation ($40 \text{ nm} - 2.5 \text{ }\mu\text{m}$), and coarse mode ($>2.5 \text{ }\mu\text{m}$),
13 respectively. Many studies indicate that there are large difference between existing
14 theoretical and observed size-resolved washout rates (Wang et al., 2010; Andronache et
15 al., 2006; Henzing et al., 2006; Laakso et al., 2003). For particles within the diameter
16 range of $0.01 - 2 \text{ }\mu\text{m}$, size-resolved washout rates derived from analytical formulas are one
17 to two orders of magnitude smaller than those derived from field measurements (e.g.,
18 Wang et al., 2010). This large difference could result from turbulent flow fluctuations
19 (Andronache et al. 2006; Khain and Pinsky, 1997), vertical diffusion process (Zhang et al.,
20 2004), and droplet-particle collection mechanisms (Park et al., 2005).

21 In GC12, Λ and b for aerosols are parameterized as a function of particle size modes
22 (Wang et al., 2011), following Feng (2007). For nitric acid, GC12 keeps $\Lambda = 1 \text{ cm}^{-1}$ and b
23 $= 1$, unchanged from the original CEOS-Chem parameters. In this study, we employ the
24 size-dependent aerosol washout parameterization derived from six years of field
25 measurements over forests in southern Finland (Laakso et al., 2003; Wang et al., 2010).
26 We further estimate nitric acid washout scavenging coefficients by referring to field

1 measurements for particles of 10 nm (Laakso et al., 2003) and the theoretical dependence
2 of scavenging coefficients on particle sizes for particles < 10 nm (Henzing et al., 2006).
3 The collection efficiency of particles smaller than 10 nm by rain droplets is dominated by
4 Brownian diffusion, and in this regard we can treat nitric acid as a single molecule (or
5 particle) with diameter of 0.5 nm. Through this approach, we derive empirical K_{wash} value
6 for nitric acid to be $3 \times 10^{-3} \text{ s}^{-1}$ when rain rate is 1 mm h^{-1} . This empirical value is about
7 two orders of magnitude larger than the corresponding K_{wash} value in GC12 ($0.1 \text{ hr}^{-1} = 2.8$
8 $\times 10^{-5} \text{ s}^{-1}$). For the dependence of K_{wash} on rain rate, we adopt the b value of 0.62 for
9 nucleation mode particles (diameter 1 nm – 40 nm) (Feng, 2007) for nitric acid. With this
10 empirical b value of 0.62 and empirical K_{wash} of $3 \times 10^{-3} \text{ s}^{-1}$, we derive an empirical Λ
11 value for nitric acid of 2. It should be noted that the unit of empirical Λ is not cm^{-1} when
12 b is not unity. In our parameterization (Eq. 8), $\Lambda=2$ and P_r should be in the unit of cm s^{-1} .
13 Washout rates for water soluble aerosols are using the empirical values from Laakso et al.
14 (2003), while washout rates for water insoluble aerosols are still using the values from
15 Feng (2007). No change is made to washout by snow, which is based on the approach
16 described in Wang et al. (2011).

17 For convective precipitation, scavenging in convective updrafts are coupled with
18 convective transport (e.g., Liu et al., 2001). Furthermore, MERRA2 meteorological fields
19 do not provide convective cloud fraction and cloud water content. Therefore, the updated
20 wet scavenging method discussed above for stratiform precipitation cannot be directly
21 applied to convective precipitation rainout scavenging in GEOS-Chem. However, the
22 empirical values for water soluble aerosol and nitric acid washout are also applied to
23 convective washout in the present study as Case 4.

24

25 **3. Model simulations and results**

26 To study the impacts of various updates to the wet scavenging as described in
27 Section 2 on model simulated nitric acid, nitrate, and ammonium mass concentrations, we

1 run GEOS-Chem for 4 cases: (1) standard GC12 parameterizations for rainout and
2 washout, called GC12; (2) same as the Case GC12 except k_{new} in Eq. 3 is used, called
3 Knew; (3) same as the Case Knew except $ICCW_t$ from MERRA2 (Eq. 4) is used, called
4 $ICCW_t$; (4) same as the Case $ICCW_t$ except empirical washout rates for nitric acid and
5 water soluble aerosols are used, called $ICCW_t_{EW}$. For each case, we carry out
6 simulations from December 2010 to December 2011, with the first month as spin-up. The
7 model horizontal resolution is $2^\circ \times 2.5^\circ$ and vertically there are 47 layers. The present
8 analysis focuses on the continental United States. We compared simulated nitric acid with
9 in-situ observations at Clean Air Status and Trends Network (CASTNET) sites, simulated
10 nitrate and ammonium with in-situ observations at Interagency Monitoring of Protected
11 Visual Environments (IMPROVE) and Chemical Speciation Network (CSN) sites. For
12 2011, there were 74 sites with available nitric acid observations from CASTNET. For the
13 same year, IMPROVE had 120 sites with available nitrate and ammonium observations,
14 while CSN had 94 sites with available nitrate observations and 63 sites with available
15 ammonium observations.

16 The effects of different modifications to the GC12 wet scavenging parameterization
17 on model simulated nitric acid, nitrate, and ammonium mass concentrations are shown in
18 Figures 2-3 and Table 1. Most of the changes of mass concentrations of the 3 species over
19 the US are caused by the changes of cloud condensation variability and/or empirical
20 washout rate. The impact of new rainout loss rate (k_{new}) is relatively small because of the
21 cancelling effect of k in the denominator and also in the exponent in Eq. 1. As shown in
22 Figs. 2a-2b and Table 1, all cases except $ICCW_t_{EW}$ overestimate nitric acid at
23 CASTNET sites by a factor 2–3 in both wintertime and summertime. Consideration of
24 cloud condensation water variability slightly reduces nitric acid in January and December
25 but has negligible effect during other months. The inclusion of the empirical washout rate
26 reduces the normalized mean bias (NMB) of nitric acid from 125 % to 24 % (Table 1).
27 Figures 2c and 2d show the impacts of improved wet scavenging on nitrate. It is clear that

1 GC12 significantly overestimates nitrate concentration at most sites especially during the
2 wintertime, in agreement with previous studies (Heald et al., 2012; Walker et al., 2012).
3 Replacing constant ICCW with variable $ICCW_t$ reduces the NMB of nitrate from 170 %
4 to 84 %. ICCW has significant impact on reducing nitrate mass concentration during the
5 wintertime and a smaller impact during the summertime. Wintertime bias of nitrate was
6 reduced from $2 \mu\text{g m}^{-3}$ to $0.7 \mu\text{g m}^{-3}$. The change of washout rate from theoretical value
7 to empirical formula results in an additional 59 % reduction of NMB for nitrate and
8 impacts nitrate mass concentration significantly both in the winter and in the summer. For
9 ammonium, NMB is reduced from 85 % to 43 % after considering rainout with variable
10 cloud condensation water. Similar to nitrate, the impact of ICCW is large during the
11 wintertime and smaller during the summer time. After considering empirical washout, the
12 NMB of ammonium is reduced to 13 %. While the update in the wet scavenging
13 parameterization significantly improves agreement of the model simulated mass
14 concentrations of nitric acid, nitrate, and ammonium over the US with those observed, it
15 does not affect the correlation coefficients of annual mean values (Table 1) which are
16 dominated by spatial distributions (Fig. 3).

17 Figure 3 shows the horizontal distributions of surface layer nitric acid, nitrate, and
18 ammonium mass concentrations over the US for case GC12 (a-c) and case $ICCW_t_EW$
19 (d-f). For comparison, annual mean mass concentrations observed at CASTNET,
20 IMPROVE, and CSN sites are shown in filled circles. The spatial pattern of the simulated
21 concentrations of the three species for the $ICCW_EW$ case is close to those for the GC12
22 case. High concentrations of nitric acid are mainly located at northeastern, southern, and
23 western US with the values up to $2-4 \mu\text{g m}^{-3}$ based on GC12 (Fig. 3a) and $1-2 \mu\text{g m}^{-3}$
24 based on $ICCW_t_EW$ (Fig. 3d). Horizontal distribution of nitrate is different from that of
25 nitric acid. Nitrate is mainly located at the Ohio valley region and the Northeastern US
26 with values up to $4-5 \mu\text{g m}^{-3}$ based on GC12 (Fig. 3b) and $1-3 \mu\text{g m}^{-3}$ based on
27 $ICCW_t_EW$ (Fig. 3e). Ammonium shows a similar horizontal distribution to that of

1 nitrate, but its value is ~50 % lower than nitrate concentration. For the whole continental
2 US domain, the annual mean nitric acid, nitrate, and ammonium concentration in the
3 model surface layer are reduced from 1.48 $\mu\text{g m}^{-3}$ to 0.78 $\mu\text{g m}^{-3}$, 1.03 $\mu\text{g m}^{-3}$ to 0.46 μg
4 m^{-3} , 0.76 $\mu\text{g m}^{-3}$ to 0.47 $\mu\text{g m}^{-3}$, respectively. The percentage changes for nitric acid,
5 nitrate, and ammonium concentrations averaged within the domain are -47%, -55%, and
6 -38%, respectively. The improved wet scavenging treatment had significant impacts on
7 nitric acid, nitrate, and ammonium modeling over the US. As can be seen from Figs.
8 3a-3f (and also Fig. 2 and Table 2), simulated nitric acid, nitrate, and ammonium mass
9 concentrations over the US based on the updated wet scavenging parameterization (i.e.,
10 ICCW_tEW) are in much better agreement with in-situ measurements.

11

12 **4. Summary and discussions**

13 We present an improved wet scavenging parameterization for using in GEOS-Chem
14 by considering cloud condensation water variability and an empirical washout rate. The
15 updated parameterization significantly reduces the overestimation of simulated annual
16 mean mass concentrations of nitric acid, nitrate, and ammonium at CASTNET,
17 IMPROVE, and CSN sites in US, from 2.04 to 1.03 (observation: 0.83) $\mu\text{g m}^{-3}$, 1.89 to
18 0.88 (observation: 0.70) $\mu\text{g m}^{-3}$, 1.09 to 0.68 (observation: 0.60) $\mu\text{g m}^{-3}$, respectively. In
19 addition, the agreement of model simulated seasonal variations of corresponding species
20 with measurements is also improved. The updated wet scavenging scheme provides a
21 partial solution to the persistent problem of nitric acid and nitrate overestimation in the
22 widely used community model GEOS-Chem (e.g., Heald et al., 2012) and thus improve
23 the skill of the model in predicting nitric acid, nitrate, and ammonium concentrations. It
24 should be noted that in the present study the cloud condensation water variability is
25 considered only for stratiform cloud rainout. Convective cloud removal is important
26 (especially for tropical regions) and is necessary to be studied as well, calling for the
27 output of convective cloud fraction and cloud water content fields in future GMAO

1 reanalysis products.

2 The empirical washout rate suggested in the present work will also help to resolve
3 the significant over-prediction of nitric acid by most of the 9 global models participating
4 in the Aerosol Comparisons between Observations and Models (AeroCom) phase III
5 study (Bian et al., 2017). Due to large difference in nitric acid washout rate based on
6 theoretical and field studies and the importance of this rate, further research is needed to
7 better understand the underlying reasons and reduce the difference. At the time being, we
8 recommend the empirical values to be used in models. The revised rainout scheme
9 presented in this study can be applied to other atmospheric chemistry models assuming
10 constant cloud condensation water. The changes of nitrate and ammonium mass
11 concentrations not only impact particle growth but also influence ammonia
12 concentrations which are important for aerosol nucleation (Kirkby et al., 2011; Yu et al.,
13 2018), via the equilibrium of sulfate-nitrate-ammonium. The updated scheme presented
14 in this study has potential implications to new particle formation, particle growth, aerosol
15 size, CCN number concentration and associated radiative forcing, which will be the
16 subjects of future research.

17 In this study, we only evaluated the impacts of the updated wet scavenging
18 parameterization on nitric acid, nitrate, and ammonium concentrations at the surface level
19 over the US. The updated wet scavenging parameterization can also impact other soluble
20 tracers. For example, as shown in the supporting material (table S1 and figure S1), the
21 applying of ICCW and empirical washout rate can reduce the simulated annual mean
22 mass concentrations of sulfate at IMPROVE and CSN sites in US from 1.56 to 1.18
23 (observation: 1.30) $\mu\text{g m}^{-3}$. The NMB is changed from 20 % to -9 %. The impacts of the
24 updated wet scavenging parameterization on the concentrations all major aerosols over
25 the whole globe should be carefully assessed against relevant measurements in future
26 studies. In addition, the impact of the updated treatment of wet scavenging on aerosol
27 vertical profile and mass loading shall be investigated. Previous study by Liu et al. (2001)

1 indicate that Pb-210 is a good tracer for testing wet deposition in GEOS-Chem. It will be
2 helpful to carry out Pb-210 simulation to further evaluate the updated wet scavenging
3 parameterization.

4

5 Code and data availability. The code of GEOS-Chem 12.0.0 is available through the
6 GEOS-Chem distribution web-page
7 http://wiki.seas.harvard.edu/geos-chem/index.php/GEOS-Chem_12. All measurement
8 data are publicly available.

9

10 Author contributions. GL and FY proposed and implemented the revised wet scavenging
11 scheme and validated model simulations with surface observations. JS provided useful
12 suggestions to improve this work. All authors contributed to the writing and editing of the
13 paper.

14

15 Competing interests. The authors declare that they have no conflict of interest.

16

17 Acknowledgments. This work is supported by NYSERDA under contract 100416, NASA
18 under grant NNX13AK20G, and NSF under grant 1550816. We would like to
19 acknowledge Interagency Monitoring of Protected Visual Environments (IMPROVE),
20 Chemical Speciation Network (CSN), and Clean Air Status and Trends Network
21 (CASTNET) for the in-site measurement data. GEOS-Chem is a community model
22 maintained by the GEOS-Chem Support Team at Harvard University.

23

24 **References**

25 Andronache, C., Grönholm, T., Laakso, L., Phillips, V., and Venäläinen, A., Scavenging
26 of ultrafine particles by rainfall at a boreal site: observations and model estimations,
27 *Atmos. Chem. Phys.*, 6, 4739-4754, <https://doi.org/10.5194/acp-6-4739-2006>, 2006.

1 Backes, A., Aulinger, A., Bieser, J., Matthias, V., Quante, M., Ammonia emissions in
2 Europe, part I: development of a dynamical ammonia emission inventory. *Atmos.*
3 *Environ.* 131, 55–66, 2016.

4 Bauer, S. E., Koch, D., Unger, N., Metzger, S. M., Shindell, D. T., and Streets, D. G.:
5 Nitrate aerosols today and in 2030: a global simulation including aerosols and
6 tropospheric ozone, *Atmos. Chem. Phys.*, 7, 5043-5059,
7 <https://doi.org/10.5194/acp-7-5043-2007>, 2007.

8 Beheng, K. D. and G. Doms, A general formulation of collection rates of cloud and
9 raindrops using the kinetic equation and comparison with parameterizations. *Beitr.*
10 *Phys. Atmos.*, 59, 66–84, 1986.

11 Bey, I., D. J. Jacob, R. M. Yantosca, J. A. Logan, B. Field, A. M. Fiore, Q. Li, H. Liu, L. J.
12 Mickley, and M. Schultz, Global modeling of tropospheric chemistry with
13 assimilated meteorology: Model description and evaluation, *J. Geophys. Res.*, 106,
14 23,073 – 23,096, doi:10.1029/2001JD000807, 2001.

15 Bian, H., Chin, M., Hauglustaine, D. A., Schulz, M., Myhre, G., Bauer, S. E., Lund, M. T.,
16 Karydis, V. A., Kucsera, T. L., Pan, X., Pozzer, A., Skeie, R. B., Steenrod, S. D.,
17 Sudo, K., Tsigaridis, K., Tsimpidi, A. P., and Tsyro, S. G., Investigation of global
18 particulate nitrate from the AeroCom phase III experiment, *Atmos. Chem. Phys.*, 17,
19 12911-12940, <https://doi.org/10.5194/acp-17-12911-2017>, 2017.

20 Bosilovich, M. G., R. Lucchesi, and M. Suarez: MERRA-2: File Specification. GMAO
21 Office Note No. 9 (Version 1.1), 73 pp, available from
22 http://gmao.gsfc.nasa.gov/pubs/office_notes, 2016.

23 Croft, B., Martin, R. V., Leaitch, W. R., Tunved, P., Breider, T. J., D’Andrea, S. D., and
24 Pierce, J. R.: Processes controlling the annual cycle of Arctic aerosol number and
25 size distributions, *Atmos. Chem. Phys.*, 16, 3665-3682,
26 <https://doi.org/10.5194/acp-16-3665-2016>, 2016.

27 Feng, J., A 3-mode parameterization of below-cloud scavenging of aerosols for use in

1 atmospheric dispersion models, *Atmos. Environ.*, 41, 6808–6822, 2007.

2 Fountoukis, C., and A. Nenes, ISORROPIA II: A computationally efficient
3 thermodynamic equilibrium model for
4 K^+ - Ca^{2+} - Mg^{2+} - NH_4^+ - Na^+ - SO_4^{2-} - NO_3^- - Cl^- - H_2O aerosols, *Atmos. Chem. Phys.*,
5 7(17), 4639-4659, 2007.

6 Giorgi, F., and W. L. Chameides, Rainout lifetimes of highly soluble aerosols and gases
7 as inferred from simulations with a general circulation model, *J. Geophys. Res.*,
8 91(D13), 14367–14376, doi:10.1029/JD091iD13p14367, 1986.

9 Heald, C. L., Collett Jr., J. L., Lee, T., Benedict, K. B., Schwandner, F. M., Li, Y., Clarisse,
10 L., Hurtmans, D. R., Van Damme, M., Clerbaux, C., Coheur, P.-F., Philip, S., Martin,
11 R. V., and Pye, H. O. T., Atmospheric ammonia and particulate inorganic nitrogen
12 over the United States, *Atmos. Chem. Phys.*, 12, 10295–10312,
13 <https://doi.org/10.5194/acp-12-10295-2012>, 2012.

14 Henzing, J. S., Oliviere, D. J. L., and van Velthoven, P. F. J., A parameterization of size
15 resolved below cloud scavenging of aerosol by rain, *Atmos. Chem. Phys.*, 6,
16 3363–3375, doi:10.5194/acp-6-3363-2006, 2006.

17 Jacob, D. J., Liu, H., Mari, C., and Yantosca, B. M., Harvard wet deposition scheme for
18 GMI,
19 acmg.seas.harvard.edu/geos/wiki_docs/deposition/wetdep.jacob_etal_2000.pdf,
20 2000.

21 Keller, C. A., M. S. Long, R. M. Yantosca, A. M. Da Silva, S. Pawson, and D. J. Jacob,
22 HEMCO v1.0: A versatile, ESMF-compliant component for calculating emissions in
23 atmospheric models, *Geosci. Model Devel.*, 7, 1409-1417, 2014.

24 Khain, A. P. and Pinsky, M. B., Turbulence effects on the collision kernel, II: Increase of
25 the swept volume of colliding drops, *Q. J. Roy. Meteor. Soc.*, 123, 1543–1560, 1997.

26 Kirkby, J. and co-authors, Role of sulphuric acid, ammonia and galactic cosmic rays in
27 atmospheric aerosol nucleation, *Nature*, 476, 429–433, 2011.

- 1 Laakso, L., Grönholm, T., Rannik, U., Kosmale, M., Fiedler, V., Vehkamäki, H., and
2 Kulmala, M., Ultrafine particle scavenging coefficients calculated from 6 years field
3 measurements, *Atmos. Environ.*, 37, 3605–3613, 2003.
- 4 Liu, H. Y., Jacob, D. J., Bey, I., and Yantosca, R. M., Constraints from Pb-210 and Be-7
5 on wet deposition and transport in a global three-dimensional chemical tracer model
6 driven by assimilated meteorological fields, *J. Geophys. Res.-Atmos.*, 106,
7 12109–12128, 2001.
- 8 Martin, R. V., Jacob, D. J., Yantosca, R. M., Chin, M., and Ginoux, P., Global and
9 regional decreases in tropospheric oxidants from photochemical effects of aerosols, *J.*
10 *Geophys. Res.*, 108, 4097, doi:10.1029/2002JD002622, 2003.
- 11 Myhre, G., Samset, B. H., Schulz, M., Balkanski, Y., Bauer, S., Berntsen, T. K., Bian, H.,
12 Bellouin, N., Chin, M., Diehl, T., Easter, R. C., Feichter, J., Ghan, S. J.,
13 Hauglustaine, D., Iversen, T., Kinne, S., Kirkevåg, A., Lamarque, J.-F., Lin, G., Liu,
14 X., Lund, M. T., Luo, G., Ma, X., van Noije, T., Penner, J. E., Rasch, P. J., Ruiz, A.,
15 Seland, Ø., Skeie, R. B., Stier, P., Takemura, T., Tsigaridis, K., Wang, P., Wang, Z.,
16 Xu, L., Yu, H., Yu, F., Yoon, J.-H., Zhang, K., Zhang, H., and Zhou, C., Radiative
17 forcing of the direct aerosol effect from AeroCom Phase II simulations, *Atmos.*
18 *Chem. Phys.*, 13, 1853-1877, <https://doi.org/10.5194/acp-13-1853-2013>, 2013.
- 19 Park, S. H., Jung, C. H., Jung, K. R., Lee, B. K., and Lee, K. W., Wet scrubbing of
20 polydisperse aerosols by freely falling droplets, *Aerosol Sci.*, 36, 1444–1458, 2005.
- 21 Pye, H. O. T., H. Liao, S. Wu, L. J. Mickley, D. J. Jacob, D. K. Henze, and J. H. Seinfeld,
22 Effect of changes in climate and emissions on future sulfate - nitrate - ammonium
23 aerosol levels in the United States, *J. Geophys. Res.*, 114, D01205, doi:
24 10.1029/2008JD010701, 2009.
- 25 Twomey, S., The influence of pollution on the shortwave albedo of clouds, *J. Atmos. Sci.*,
26 34, 1149–1152, 1977.
- 27 Walker, J., M., Philip, S., Martin, R. V., and Seinfeld, J. H., Simulation of nitrate, sulfate,

1 and ammonium aerosols over the United States, *Atmos. Chem. Phys.*, 12,
2 11213–11227, <https://doi.org/10.5194/acp-12-11213-2012>, 2012.

3 Wang, Q., D.J. Jacob, J.A. Fisher, J. Mao, E.M. Leibensperger, C.C. Carouge, P. Le Sager,
4 Y. Kondo, J.L. Jimenez, M.J. Cubison, and S.J. Doherty, Sources of carbonaceous
5 aerosols and deposited black carbon in the Arctic in winter-spring: implications for
6 radiative forcing, *Atmos. Chem. Phys.*, 11, 12,453-12,473, 2011.

7 Wang, X., Zhang, L., and Moran, M. D., Uncertainty assessment of current size-resolved
8 parameterizations for below-cloud particle scavenging by rain, *Atmos. Chem. Phys.*,
9 10, 5685-5705, <https://doi.org/10.5194/acp-10-5685-2010>, 2010.

10 Yu, F., Nadykto, A. B., Herb, J., Luo, G., Nazarenko, K. M., and Uvarova, L. A.,
11 H₂SO₄–H₂O–NH₃ ternary ion-mediated nucleation (TIMN): kinetic-based model
12 and comparison with CLOUD measurements, *Atmos. Chem. Phys.*, 18,
13 17451-17474, <https://doi.org/10.5194/acp-18-17451-2018>, 2018.

14 Yu, F. and Luo, G., Simulation of particle size distribution with a global aerosol model:
15 contribution of nucleation to aerosol and CCN number concentrations, *Atmos. Chem.*
16 *Phys.*, 9, 7691-7710, <https://doi.org/10.5194/acp-9-7691-2009>, 2009.

17 Zakoura M. and S.N. Pandis, Overprediction of aerosol nitrate by chemical transport
18 models: The role of grid resolution. *Atmos. Environ.* 187, 390-400, 2018.

19 Zhang, L., Jacob, D.J., Knipping, E.M., Kumar, N., Munger, J.W., Carouge, C.C., Van
20 Donkelaar, A., Wang, Y.X., Chen, D., Nitrogen deposition to the United States:
21 distribution, sources, and processes. *Atmos. Chem. Phys.* 12, 4539–4554, 2012.

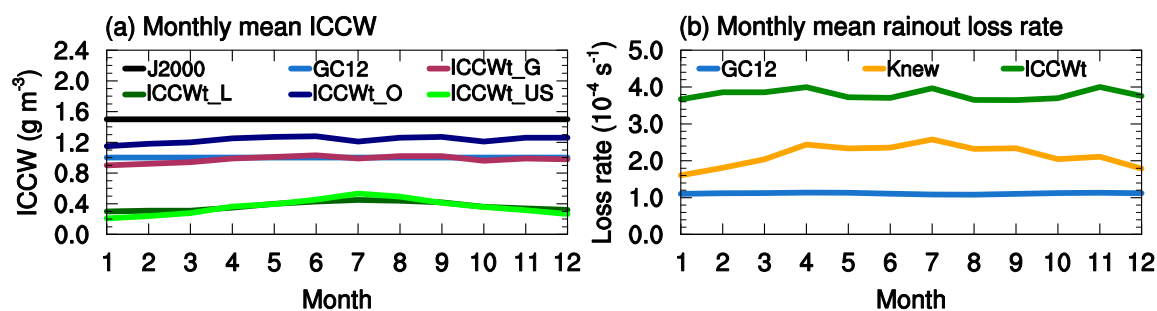
22 Zhang, L., Michelangeli, D. V., and Taylor, P. A., Numerical studies of aerosol
23 scavenging in low-level, warm stratiform clouds and precipitation, *Atmos. Environ.*,
24 38, 4653–4665, 2004.

25

1 Table 1. Observed annual mean surface concentrations of HNO₃, nitrate, and ammonium
 2 at CASTNET, IMPROVE, and CSN sites. Annual mean surface concentrations (Mean),
 3 normalized mean bias (NMB), and correlation coefficient (*r*) between observed and
 4 simulated annual mean values for the 3 species by GC12, Knew, ICCW_t, and ICCW_t_EW
 5 cases.

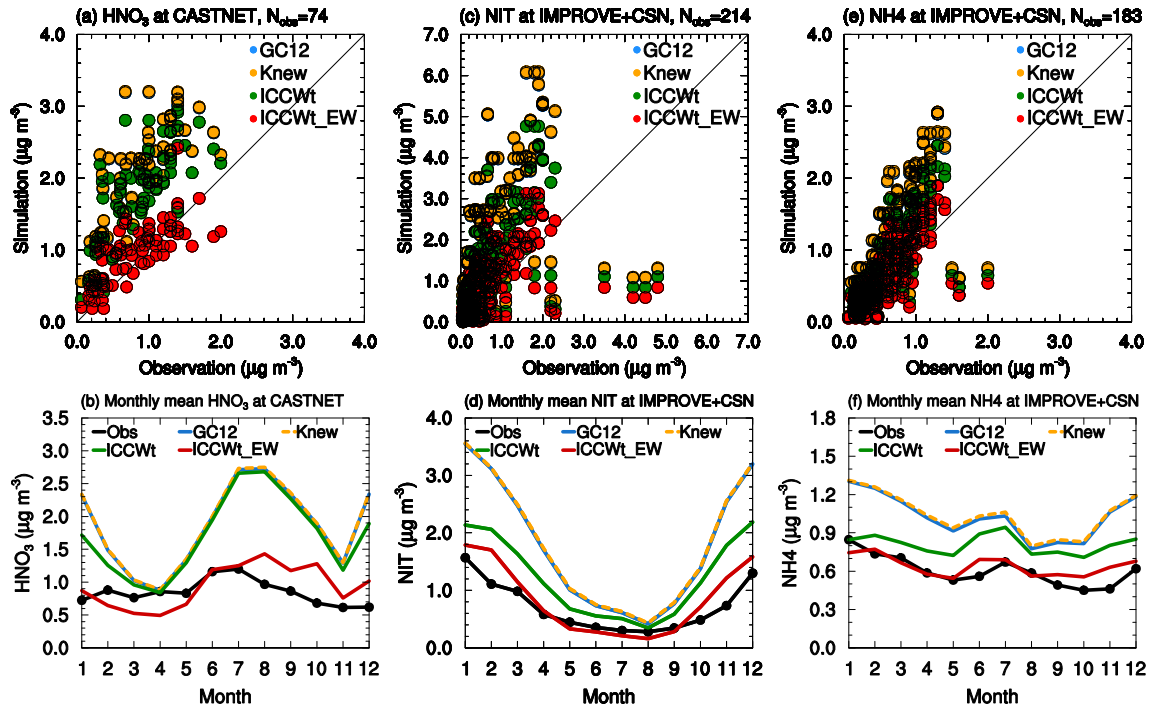
	HNO ₃			NIT			NH ₄		
	Mean (μg m ⁻³)	NMB (%)	<i>r</i>	Mean (μg m ⁻³)	NMB (%)	<i>r</i>	Mean (μg m ⁻³)	NMB (%)	<i>r</i>
Observation	0.83			0.70			0.60		
GC12	2.04	145.1	0.73	1.89	168.1	0.53	1.09	81.4	0.75
Knew	2.05	146.8	0.73	1.90	170.5	0.53	1.11	84.5	0.75
ICCW _t	1.87	125.0	0.74	1.29	83.5	0.57	0.86	42.7	0.78
ICCW _t _EW	1.03	24.2	0.72	0.88	25.0	0.57	0.68	12.8	0.78

6
7
8



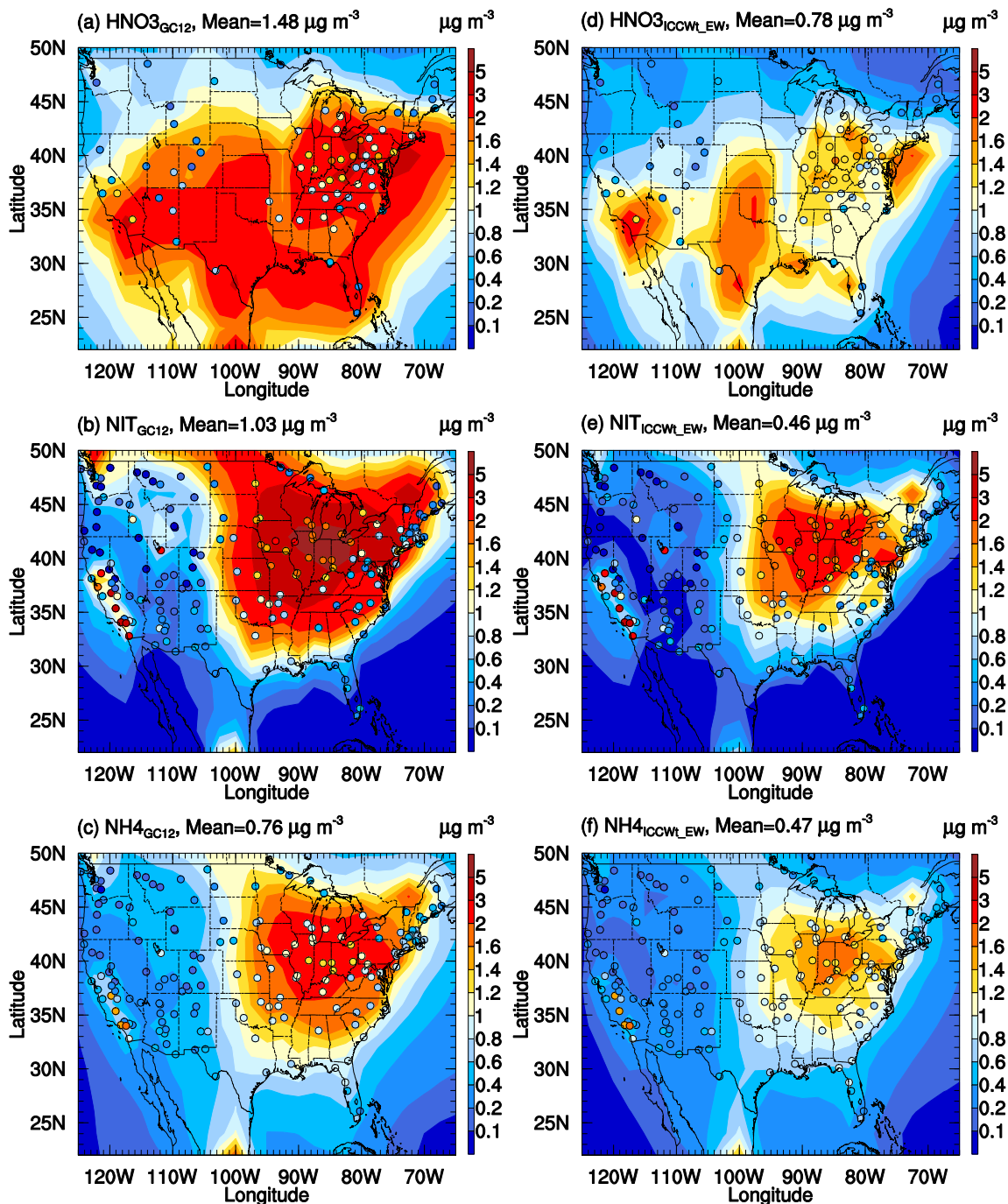
9

10 Figure 1. (a) Monthly variations of ICCW averaged over the lower troposphere layers of
 11 the whole globe (maroon), global land areas (olive), global oceans (navy), and
 12 continental US (green) from MERRA2, along with constant ICCW values assumed in
 13 J2000 (black) and GC12 (blue). (b) Monthly variations of the rainout loss rate averaged
 14 in the lower troposphere layers of the continental US based on Eq. (2) (i.e, GC12) and Eq.
 15 (3) with constant ICCW of 1 g m⁻³, and Eq. (3) with MERRA2 ICCW (Eq. 4).
 16



1
 2 Figure 2. (a) Scatter plot of observed and simulated annual mean HNO_3 at CASTNET
 3 sites and (b) variations of monthly mean for year 2011 showing the comparison between
 4 nitric acid mass concentrations observed at CASTNET sites (black) and simulated by
 5 GC12 (blue), Knew (yellow dash), ICCW_t (green), and ICCW_tEW (red) cases. (c) and
 6 (d) are the same as (a) and (b) but for nitrate at IMPROVE+CSN sites. (e) and (f) are the
 7 same as (a) and (b) but for ammonium at IMPROVE+CSN sites. It is worthy of note that
 8 the differences between G12 (blue) and Knew (yellow dash) are small.

9



1

2 Figure 3. Horizontal distributions of surface layer nitric acid, nitrate, and ammonium
 3 simulated by the GC12 case (a-c) and the ICCW_t_EW case (d-f). Filled circles are annual
 4 mean surface mass concentrations observed at CASTNET, IMPROVE, and CSN for
 5 corresponding species.